Tribol Lett (2015) 59:7
DOI 10.1007/s11249-015-0531-4

ORIGINAL PAPER

Effects of vdW Interaction and Electric Field on Friction in MoS_2

Changqing Wang[1,2] · Weiguang Chen[3] · Yongsheng Zhang[2] · Qiang Sun[1] · Yu Jia[1]

Received: 16 January 2015 / Accepted: 8 April 2015 / Published online: 22 May 2015

Abstract Sliding behaviors between two MoS_2 layers have been investigated using DFT calculations including vdW dispersion. Contribution of vdW interactions to energy corrugations and maximum lateral frictional forces of the sliding system has been calculated. Our investigations show that the smaller the external normal load is, the larger the contribution of vdW interaction to the friction is. The energy corrugation and lateral frictional force as a function of the electric field are derived, suggesting that friction can be reduced by an external electric field. The reduced friction is attributed to a weaker chemical interaction enabled by the charge depletion between the adjacent S planes. In-depth understanding of the relationship between friction and interlayer interaction shows that friction can be tuned by external electric fields.

Keywords First principles · Friction · Sliding · MoS_2 · Electric field · vdW interaction

1 Introduction

Thanks to recent developments in nanotechnology, the hope is high to build mechanical devices on the scale of the nanometer. For this purpose, it is important to determine the mechanical and, especially, frictional properties in such nanodevices. The understanding and control of frictional properties of matter at the nanoscale remain a great challenge for a wide spectrum of sciences, ranging from engineering studies of micromachine lubrication to atomistic simulations of nanoscale systems. In particular, microelectro-mechanical system (MEMS) and nanoelectromechanical system (NEMS) devices hold a tremendous potential in a variety of applications. One important challenge in applications of MEMS devices is that at these small scales, surface forces, e.g., adhesion and friction, become dominant and can lead to a fast degradation of material's performance. Therefore, fundamental understanding of friction at the atomic scale is essential for the successful design of MEMS and NEMS devices [1, 2].

Among the various members of the transition metal dichalcogenides (TMDs) family of compounds, MoS_2, usually used as a solid lubricant in MEMS, is well known for its lubricating behavior [3–5]. Its lubricating behavior stems from easy glide between MoS_2 sheets which is intrinsic to its crystal structure. Similar to graphite, MoS_2 crystallizes in the hexagonal structure where a sheet of molybdenum atoms is sandwiched between two hexagonally packed sulfur layers. The bonding within the S–Mo–S sandwich is covalent, while weak van der Waals forces hold the sandwich together resulting in interlamellar easy glide. Experimentally, pure MoS_2 can obtain a superlow friction coefficient of 0.002 (superlubricity) under high vacuum [6]. Lee et al. [2], using friction force microscopy, have investigated the nanoscale frictional characteristics of atomically thin MoS_2 sheets and found that friction monotonically increased as the number of layers decreased. The alloying MoS_2 into much harder matrices such as amorphous carbon greatly stimulates the production of efficient self-lubricating coatings [3]. Singer et al.

✉ Yu Jia
jiayu@zzu.edu.cn

[1] International Joint Research Laboratory for Quantum Functional Materials of Henan, Center for Clean Energy and Quantum Structures, School of Physics and Engineering, Zhengzhou University, Zhengzhou, Henan 450001, China

[2] Department of Mathematics and Physics, Luoyang Institute of Science and Technology, Luoyang 471023, China

[3] School of Physics and Electronic Engineering, Zhengzhou Normal University, Zhengzhou, Henan 450044, China

[7] have reported the friction coefficient of thin MoS_2 coatings decreases as the load increases. Moreover, the Amontons–Coulomb law has been observed on the nanoscale, when a MoS_2 flake moves on a MoS_2 surface [8]. All these evidences imply the need for a clear understanding of its tribological properties at the atomistic level, and particular attention must also be paid to unraveling the nature of the interlayer forces, as an interplay of electrostatic interactions, van der Waals (vdW) forces, and Pauli repulsion [2, 9–12]. In recent years, compared to tremendous attention paid to layered MoS_2 with exceptional electronic, optical, and catalytic properties (see review [13–15]), less work [9, 16–21] studied its tribological behavior. Previously, the static potential energy surfaces and atomic-scale energetic barriers encountered during sliding at MoS_2 (0001) and MoO_3 (001) surfaces and at the MoS_2/MoO_3 interface have been firstly calculated by using first-principles method [16]. The results suggest that the lowest energy pathway is to slide MoO_3 over MoS_2, and the highest energy pathway involves MoO_3 (001) interlayer sliding. Blumberg et al. [18] also determined the sliding potential of MoS_2 by a simple and intuitive explanation on the basis of the registry index (RI) concept. Onodera et al. [9] found that the predominant interaction between two MoS_2 sheets is Coulombic repulsion, which directly affects the MoS_2 lubrication using a computational chemistry method. Moreover, this group has investigated the friction anisotropy of two-layered MoS_2 at atomistic level adopting the same method [17].

The first-principles method is widely recognized as a powerful tool to examine electronic structures and the interactions between surfaces at the atomistic scale. Moreover, within the generalized gradient approximation (GGA) calculations including van der Waals corrections, the frictional figure of merit for a pair of layered MoS_2 nanostructures has been determined by Cahangirov et al. [19]. Very recently, by means of ab initio modeling of the static potential energy surface and charge distribution analysis, Levita et al. [20] demonstrated how electrostatic interactions, negligible in comparison with van der Waals and Pauli contributions at zero load, progressively affect the sliding motion at increasing loads. Our group first investigated the effect of strain on atomic-scale friction in layered MoS_2 [21]. The results indicate that one can change the interfacial interactions and then tune the interlayer friction by applying biaxial in-plane strains to the layered MoS_2. However, all the above researches have not directly studied vdW interactions between the MoS_2 layers, especially at increasing loads. The past investigations showed that vdW interactions play an important role on the electronic structures [12], the interaction energy of layered materials [22, 23], and negative friction coefficient at low load [24, 25]. Thus, there are important practical significances to investigate vdW interactions between the lamellar nanostructures at increasing loads. Moreover, Park et al. [26] reported a method by the use of electric fields for controlling friction in a nanoscale contact. They worked with a silicon pn junctions. When a bias of +4 V was applied to the sample, an increase in friction by up to a factor of 2 was observed in the p-doped region. The mechanism for this increase is not clear, but estimates of the contribution due to electronic friction (the drag force that results when charge carriers move in an electric field) are too low to explain the result. Previous investigations reveal that the friction can be tuned by modifying atomic and then electronic structures of the sliding surfaces [21, 27–30]. Moreover, one can change the electronic structure of bilayer MoS_2 by vertical electric field [31, 32]. In a word, it is necessary to study the effect of the external electric field on the sliding properties in the layered materials.

In this paper, for the purpose of better understanding the frictional behaviors between MoS_2 layers, particularly vdW interactions and effects of the external electric field, we investigate their influence on the interlayer sliding using density functional theory (DFT) calculations including vdW correction. This static approach will help providing a rationale of the microscopic processes which could lead to further insights into the tunability of the macroscopic frictional properties of MoS_2. In-depth understanding of the relationship between the atomic-scale friction and the interfacial interaction shows that the interlayer friction in MoS_2 can be tuned by external electric fields. Moreover, as the load decreases, the contribution of the vdW interactions to the friction increases. These investigations may be helpful for friction control, as well as electronic device and lubricant design.

2 Details of Calculation Methods

All of calculations in this work were performed using the Vienna ab initio simulation package (VASP) code [33, 34], equipped with the projector augmented-wave (PAW) method [35, 36] for electro-ion interaction. The exchange–correlation functional is represented with the GGA in the form of the Perdew–Burke–Ernzerhof (PBE) [37]. The electronic wave functions are expanded in a plane-wave basis with the energy cutoff of 500 eV to converge the relevant quantities. Total energy and electronic structures of the systems are calculated using a $15 \times 15 \times 1$ Monkhorst–Pack (MP) grid [38]. The convergence for energy is chosen to be 10^{-5} eV between two electronic relaxation steps, and the maximum force allowed on each atom is <0.005 eV/Å upon ionic relaxation. For an accurate description of the geometric and electronic structure of

molybdenum disulfide, we carried out DFT calculations including van der Waals dispersion forces (DFT-D2) proposed by Grimme [39].

As shown in Fig. 1, a supercell used in the present study consists of two layers of MoS_2 sheets to simulate their relative sliding. To eliminate the interactions between adjacent supercells, we consider the supercell with a length of 30 Å in the z direction, leaving a vacuum region of more than 20 Å. The loading method is similar to that described in the previous work [21]. The potential energy surface (PES) experienced by the upper monolayer upon translation above the lower one is constructed by calculating the interlayer interaction energy for different relative lateral positions of the two layers by shifting the upper layer by a step of 0.2 Å along the x and y directions, respectively. In order to study the load effect on the friction along the considered path (x direction as shown in Fig. 1), we investigate the variation of the system energy corrugation (the difference between the maximum and minimum energies) and the maximum static lateral force under different loads. The load has been evaluated as the ratio $L = F_z/A$, between the z component of the residual force on the cell F_z and the cell area A. An external electric field with a tolerable magnitude in the range of 0.1–0.3 V/Å has been applied perpendicularly to the sheets by adding an artificial dipole sheet in the middle of the vacuum part in the periodic supercell [40].

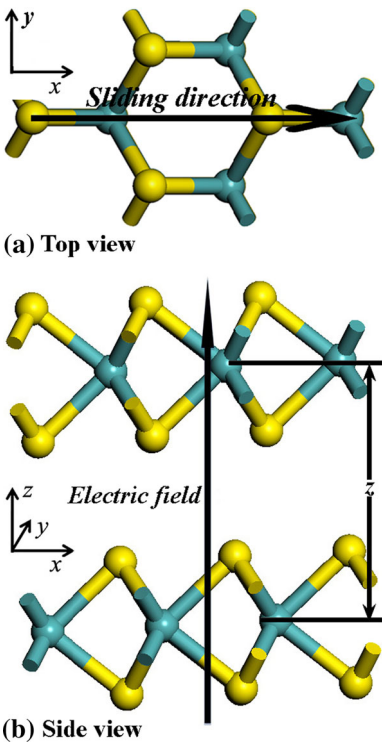

Fig. 1 *Ball* and *stick* model of MoS_2 used in the present study. *Yellow* and *aqua balls* represent S and Mo atoms, respectively. **a** Top view, **b** side view (Color figure online)

According to the DFT-D2 method [39], the total energy of a system is given by

$$E = E_c + E_{\mathrm{vdW}} \tag{1}$$

where E_c is the usual self-consistent Kohn–Sham energy and E_{vdW} is the vdW dispersion correction. The dispersion energy E_{vdW} is given by

$$E_{\mathrm{vdw}} = -s_6 \sum_{i=1}^{N-1} \sum_{j=i+1}^{N} \frac{C_6^{ij}}{R_{ij}^6} \frac{1}{1 + e^{-d\left(R_{ij}/R_r - 1\right)}} \tag{2}$$

where s_6 (0.75 for PBE potential) is a global scaling factor, N represents the number of atoms in the system, C_6^{ij} is the dispersion coefficient for atom pair ij, given by $C_6^{ij} = (C_6^i C_6^j)^{1/2}$, R_{ij} denotes the interatomic distance, and R_r represents the sum of atomic van der Waals radii, respectively. d is a damping parameter (20.0 for PBE potential). The dispersion coefficient C_6 is 24.670 and 5.570 J nm^6/mol and vdW radii R_0 is 1.639 and 1.683 Å for Mo and S atoms, respectively.

The corresponding lateral frictional force along the sliding direction f is given by

$$f = \frac{\partial E}{\partial x} = \frac{\partial E_c}{\partial x} + \frac{\partial E_{\mathrm{vdW}}}{\partial x} = f_c + f_{\mathrm{vdW}} \tag{3}$$

where f_c and f_{vdW} are the contribution of the Kohn–Sham energy and the vdW interaction to the lateral frictional force, respectively.

In the lamellar system, the energy corrugation along the sliding path is mainly composed of the change in the electrostatic and the vdW interaction between atoms of the two layers, especially in the situation of quasi-static or very low velocity sliding [23]. That is,

$$\Delta E = \Delta E_c + \Delta E_{\mathrm{vdw}} \tag{4}$$

where ΔE, ΔE_c, and ΔE_{vdW} are the energy corrugation, the variation of the electrostatic interaction energy, and the vdW interactions energy, respectively. Therefore, we can evaluate the contribution of vdW interaction to the friction between the two sheets as the ratio $^{\Delta E_{\mathrm{vdW}}}/_{\Delta E}$ and $^{\Delta f_{\mathrm{vdW}}^{\max}}/_{\Delta f^{\max}}$ where $\Delta f^{\max}$ and $\Delta f_{\mathrm{vdW}}^{\max}$ are the maximum lateral frictional force and the contribution of vdW interaction, to that, respectively.

3 Results and Discussion

3.1 vdW Interaction on Friction of MoS_2 Layers

To check the efficiency of the computational method, the MoS_2 bilayer has been first optimized using the DFT-D2 method mentioned previously. Our calculations show that

the hexagonal lattice constant a_0 is 3.198 Å, the length of the Mo–S bond is 2.417 Å, the interplanar binding energy is 0.149 meV, and the thickness of MoS_2 monolayer is 3.119 Å, in good agreement with previous calculations [20]. The interlayer distance has been calculated to be 6.22 Å, which lies within a 1.5 % margin from the experimental data (6.15 Å) [2].

Without an external electric field, the static potential energy surface (PES) at zero load mapped by the contour plot as a function of relative displacement of two MoS_2 layers in the x and y directions is shown in Fig. 2a. For convenience, the contour plot is expanded with intrinsic periodicity. The minimum potential energy is set to 0 eV. From this energy surface, we can find that the potential energy surface has the same sixfold symmetry as the surface structure of MoS_2 (0001). The energetically favored path (black solid line) during sliding is shown in Fig. 2a. Such a zigzag path in the potential energy surface has been predicted in previous work [16–20] as well. The corresponding potential energy profile for the linear translation of a MoS_2 layer above a fixed one along the x direction is shown in Fig. 2b. Four characteristic potential energies (Min1, Saddle, Min2, and Max) are also marked in this figure. According to these four potential energies, their geometric configurations are shown in Fig. 2c, d, e, f, respectively. For the minimum energy configuration, Min1, the arrangement of two-layer MoS_2 is similar to its bulk structure (Fig. 2c). Namely, the Mo (S) atom of the upper layer straightly falls on top of the S (Mo) atom of the bottom one. For the other stable configuration, Min2, the Mo atom of its upper layer is faced to the Mo atom of the other layer, while the S atom of one layer is located in the sixfold symmetry center of the other one (Fig. 2e). When the S atom of one layer is faced to that of the other (Fig. 2f), the system has the maximum potential energy, 0.053 eV/cell, in agreement with the previous calculation [20].

Next, we consider the vdW interaction on the friction of MoS_2 layers. When one layer slides above the other along the x direction, the interlayer distance, vdW interaction energy, and the corresponding potential energy at three certain normal loads (0, 5, 9 GPa) are plotted in Fig. 3a, b, c, respectively. For the vdW and potential energy, they have been set to 0 eV at the initial position ($x = 0$). At the

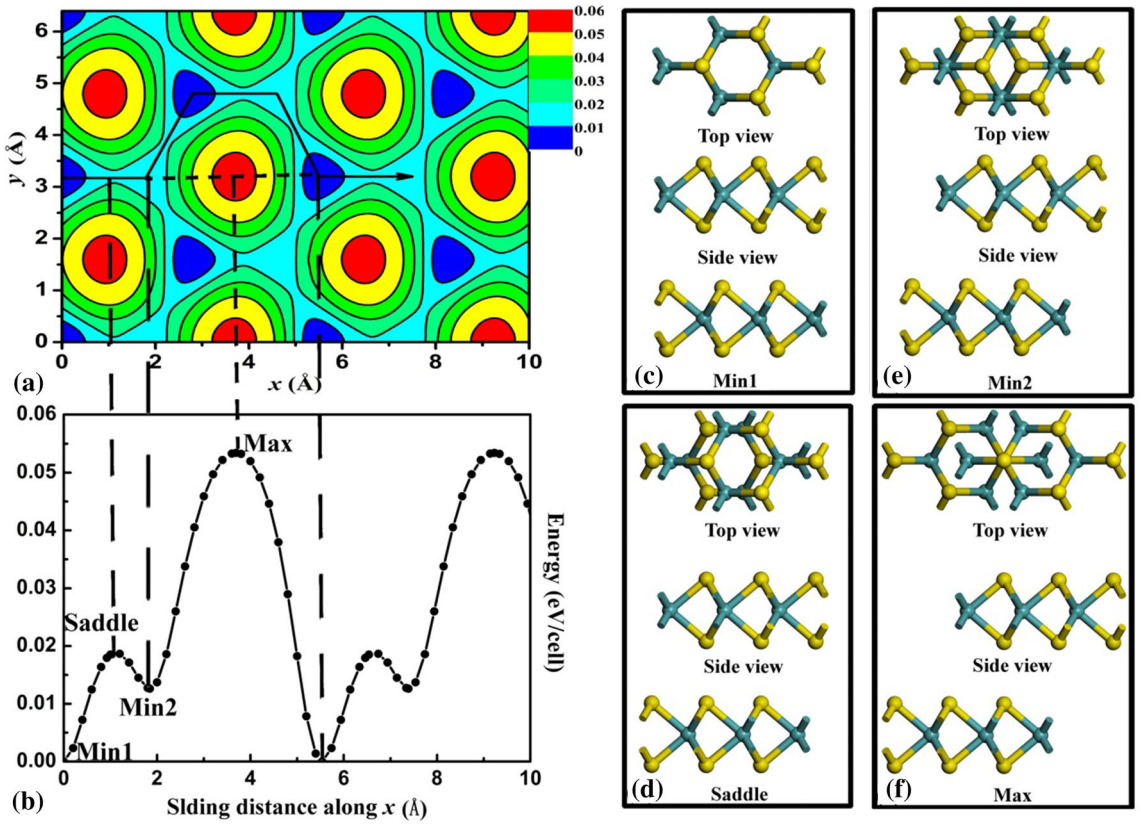

Fig. 2 **a** Potential energy surface (PES) for the sliding motion of MoS_2 bilayer at zero load. *Black solid line* represents the minimum energy path. The *color scale* refers to the energy range of the PES corrugation (in eV); **b** the potential energy profile for the linear translation of a MoS_2 layer above a fixed one along the x direction. **c**, **d**, **e**, and **f** Represents Min1, saddle, Min2, and Max geometric configuration, respectively. *Yellow* and *aqua balls* represent S and Mo atoms, respectively (Color figure online)

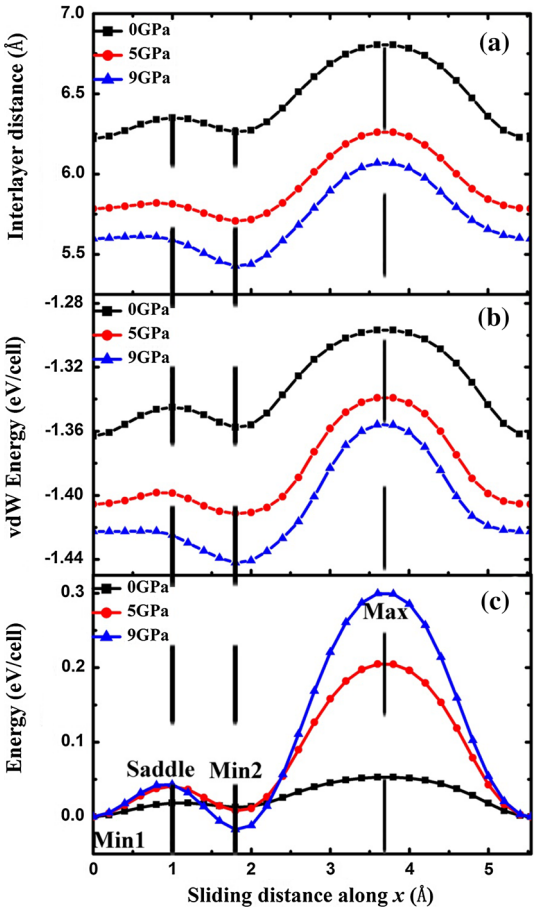

Fig. 3 Interlayer distance (**a**), vdW energy (**b**), and potential energy (**c**) as a function of the sliding distance along the x direction. The potential energy at the initial position ($x = 0$) has been set to 0 eV

same load, such as 5 GPa (red line in Fig. 3), they show a similar trend with the relative displacement of the two MoS_2 layers: The vdW interaction and potential energy increase or decrease with the increase or decrease in the interlayer distance. At a certain sliding distance (e.g., Min1, Saddle, and Max configuration), the interlayer distance and vdW interaction energy decrease with the increase in external normal load. However, due to the electrostatic repulsions between the two adjacent S planes, the potential energy raises. With respect to Min2 arrangement, its potential energy reduces with the increase in load. This may be the result of competition between van der Waals and electrostatic repulsion interactions.

Understanding of the frictional properties of MoS_2 layers requires comparing the energy corrugation and maximum lateral frictional force along the sliding path. The energy corrugations and maximum lateral frictional forces as a function of external normal loads are plotted in Fig. 4a. As the Amontons's friction law expected, both energy corrugations and maximum lateral frictional forces monotonically increase with normal loads. It shows that the

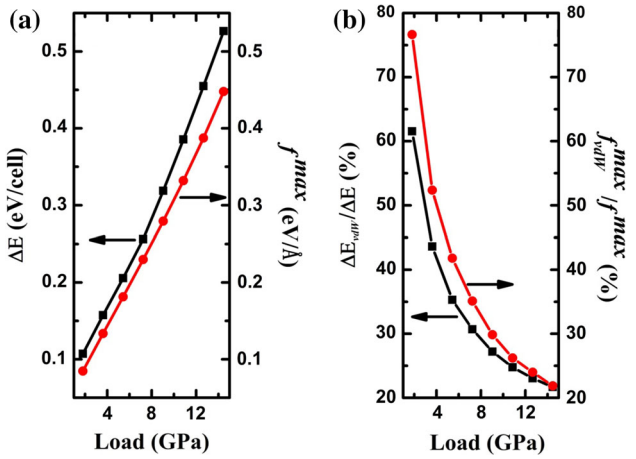

Fig. 4 **a** Energy corrugation and lateral frictional force as a function of a normal load; **b** contribution of vdW interaction to the energy corrugation and lateral frictional force as a function of a normal load

interlayer friction of MoS_2 on the atomic scale also obeys the basic friction law observed experimentally by Miura [8]. We have further studied the vdW interactions on friction of MoS_2 layers. As shown in Fig. 4b, the contributions of vdW interactions to energy corrugation and lateral frictional force as a function of a normal load have been exhibited. From the figure, we can find that vdW interactions increasingly contribute to the friction with the decreased load. Particularly, at a small load, vdW interactions dominate the interlayer friction of the sheet materials [24, 25]. Of course, the above analysis is an oversimplification of the experimental situation in which layers cannot move as rigid blocks. Instead, in a physical system, it is possible that some regions will slip, while others will not. The regions that do slip will not settle fully into their local minima and will interact elastically with other regions that have not slipped. Thus, the predicted maximum frictional forces based on this approach can be expected to be generally larger than the experimental values. These limitations notwithstanding our results give a trend in the sliding behavior as a function of a normal load, in close agreement with previous experimental measurements [8].

3.2 Effects of Electric Field on Friction of MoS_2 Layers

Among several strategies currently being employed to change electronic structures of two-dimensional materials, tuning of electronic structures by external electric fields is a particularly interesting one. Recent theoretical studies also suggest the possibility of employing a similar strategy to manipulate the band gap in bilayer MoS_2 [31, 32]. In this case, an external electric field reduces the fundamental band gap of the bilayer structure and a transition from

semiconductor to metal occurs at an appropriate situation. It is well known that the friction between two MoS_2 sheets originates from interlayer interactions. Moreover, electronic structures of the system are also sensitive to interlayer interactions. Therefore, modulation of electronic structures by electric fields may be practicable to tune the interlayer friction.

Effects of external electric fields on sliding properties of MoS_2 layers are also investigated in this paper. The electric field is perpendicularly imposed on the system by adopting an artificial dipole sheet in the middle of the vacuum (Fig. 1). Applied by an external electric field, the energy corrugation and maximum lateral frictional force of the relative sliding system at a fixed normal load have been calculated by using the above methods. Figure 5 shows the variation along the x direction of the system energy corrugation (Fig. 5a) and the maximum static lateral force (Fig. 5b) under external electric fields. Our results indicate that the energy corrugation and the corresponding maximum lateral frictional force take on a similar trend. That is, at a constant external electric field, higher energy corrugation and maximum lateral frictional force will be experienced when one layer slides relatively to another under higher load. And even it is more interesting that, compared with a zero electric field, the energy corrugation and maximum lateral frictional force at a fixed load slightly increase with the applied electric field from 0 to 0.25 eV/Å, while they decrease with a more intensive electric field (>0.25 eV/Å), in which the 0.25 eV/Å is a critical value.

In order to comprehensively understand the effects of electric fields on the friction of the two MoS_2 layers, electronic structures of this system at a fixed load need to be investigated. Firstly, energy band structures under different electric fields of the two MoS_2 layers have been calculated. In Fig. 6, we provide an overview of the band

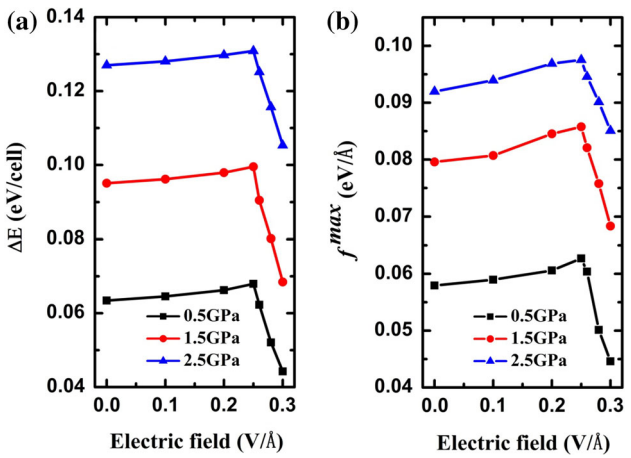

Fig. 5 Energy corrugation (**a**) and maximum lateral frictional force (**b**) at a fixed normal load as a function of the external electric field

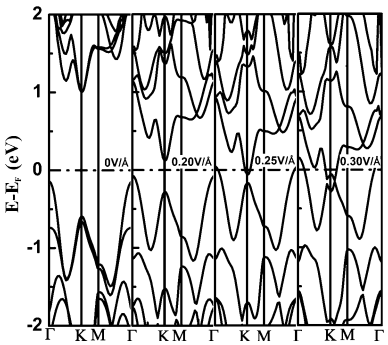

Fig. 6 Energy band structures of the MoS_2 bilayer applied with different electric fields. The normal load is 0.5 GPa. The fermi level is set to 0 eV

structures of the MoS_2 bilayer at a 0.5-GPa load considered in this work as a function of applied external field. It is apparent at a glance that the band gap in this case is driven continuously to zero with increasing external electric fields. We note that the fundamental band gap at zero electric field is an indirect gap between the valence-band (VB) maximum at Γ and the conduction-band (CB) minimum at K. The VB maxima at Γ and CB minima at K inexorably approach the Fermi energy value with increasing external electric fields. At the electric field of about 0.25 eV/Å, similar to the critical value of friction transition (Fig. 5), the bilayer translates from semiconductor to metal. The band-gap modulation discussed above arises from the well-known Stark effect, which has been observed in the previous studies as well [31, 32]. External perpendicular electric field induces a potential difference between the two layers. As a result, the energy bands belonging to different MoS_2 layers are separated from each other entirely. In MoS_2 bilayer, the stronger the electric field is, the larger the band splitting is, and thus the smaller the band gap is.

Next, the self-consistent difference of charge density is obtained by subtracting the charge density of the MoS_2 bilayer with an electric field from that of the MoS_2 bilayer without an electric field. The isosurfaces of the difference of charge density and the variation of its value averaged over (x, y) planes parallel to MoS_2 layers (called the difference of linear charge density along the z axis) are presented in Fig. 7. Generally, charge distribution of the sliding interface dominates the friction between the two relative sliding interfaces [28]. The charge density accumulation for 0.20 eV/Å (depletion for 0.30 eV/Å) between the two adjacent S planes is the key feature to explain the increase (decrease) in the energy corrugation and maximum lateral frictional force. This charge accumulation (depletion) enhances (weakens) the chemical interaction between the two layers and results in the increase (decreasing) in energy corrugation and lateral frictional force as shown in Fig. 5. Our theoretical investigations may

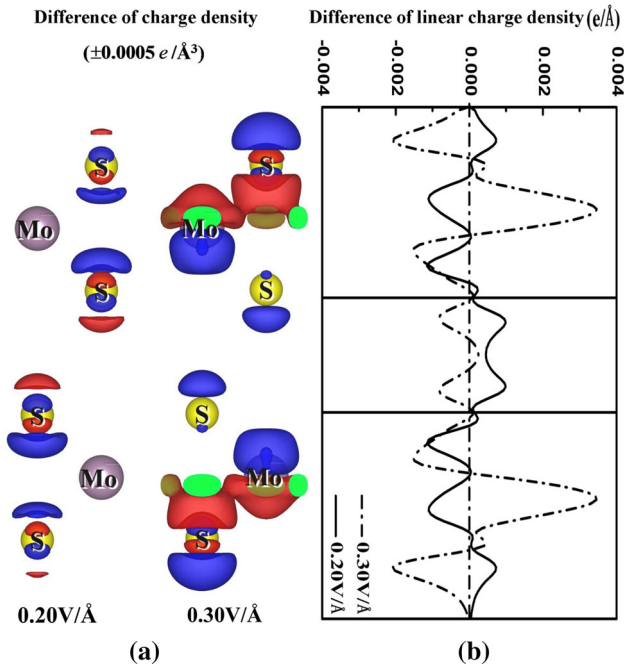

Fig. 7 **a** Difference of charge density ($\Delta\rho = 0.0005$ e/Å^3) of the MoS_2. **b** Changes in the linear charge density distribution along the z direction. The normal load is 0.5 GPa. *Red* (*blue*) isosurface plots correspond to the charge density accumulation (depletion). For the definition of difference of charge density, see the text (Color figure online)

provide important information on how to reduce friction between MoS_2 interfaces. Of course, theoretical calculations need to be verified by experiment.

4 Conclusions

Sliding properties of two MoS_2 layers have been investigated by the use of density functional theory (DFT) calculations including van der Waals corrections. Static potential energy surface of the relative sliding system is plotted in this paper. Contribution of vdW interactions to energy corrugations and maximum lateral frictional forces of the sliding system has been calculated by the DFT-D2 method. Our results show that the smaller the external normal load is, the larger the contribution of vdW interaction to the friction is. Furthermore, the energy corrugation and maximum lateral frictional force as a function of the electric field are derived as well, suggesting that the friction between two MoS_2 layers can be reduced by imposing an electric field. The reduced friction is attributed to a weaker chemical interaction enabled by the charge depletion between the adjacent S atomic planes. In-depth understanding of the relationship between friction and interfacial interaction shows that friction can be tuned with an external electric field.

Acknowledgments This work was supported by the NSF of China (Grant No. 11274280) and the Outstanding Young Foundations in Henan Province and the Science and Technology Development Plan Project of Henan Province (Grant No. 132300410085, 142300410024).

References

1. Carpick, R.W.: Controlling friction. Science **313**, 184–185 (2006)
2. Lee, C., Li, Q., Kalb, W., Liu, X., Berger, H., Carpick, R.W., Hone, J.: Frictional characteristics of atomically thin sheets. Science **328**, 76–80 (2010)
3. Polcar, T., Cavaleiro, A.: Review on self-lubricant transition metal dichalcogenide nanocomposite coatings alloyed with carbon. Surf. Coat. Technol. **206**, 686–695 (2011)
4. Scharf, T.W., Prasad, S.V.: Solid lubricants: a review. J. Mater. Sci. **48**, 511–531 (2013)
5. Li, J.J., Luo, J.B.: Advancements in superlubricity. Sci. China Technol. Sci. **56**, 2877–2887 (2013)
6. Martin, J.M., Donnet, C., Mogne, T.L.: Superlubricity of molybdenum disulphide. Phys. Rev. B **48**, 10583–10586 (1993)
7. Singer, I.L., Bolster, R.N., Wegand, J., Fayeulie, S., Stupp, B.C.: Hertzian stress contribution to low friction behavior of thin MoS_2 coatings. Appl. Phys. Lett. **57**, 995–997 (1990)
8. Miura, K., Kamiya, S.: Observation of the Amontons-Coulomb law on the nanoscale: frictional forces between MoS2 flakes and MoS_2 surfaces. Europhys. Lett. **58**, 610–615 (2002)
9. Onodera, T., Morita, Y., Suzuki, A., Koyama, M., Tsuboi, H., Hatakeyama, N., Endou, A., Takaba, H., Kubo, M., Dassenoy, F., Minfray, C., Lucile, J., Martin, J., Miyamoto, A.: A computational chemistry study on friction of h-MoS2. Part I. Mechanism of single sheet lubrication. J. Phys. Chem. B **113**, 16526–16536 (2009)
10. Cheng, Y., Zhu, Z., Schwingenschlögl, U.: Role of interlayer coupling in ultra thin MoS_2. RSC Adv. **2**, 7798–7802 (2012)
11. Yun, W.S., Han, S.W., Hong, S.C., Kim, I.G., Lee, J.D.: Thickness and strain effects on electronic structures of transition metal dichalcogenides: 2H-MX_2 semiconductors (M = Mo, W; X = S, Se, Te). Phys. Rev. B **85**, 033305 (2012)
12. Han, S.W., Kwon, H., Kim, S.K., Ryu, S., Yun, W.S., Kim, D.H., Hwang, J.H., Kang, J.S., Baik, J., Shin, H.J., Hong, S.C.: Band-gap transition induced by interlayer van der Waals interaction in MoS_2. Phys. Rev. B **84**, 045409 (2011)
13. Tang, Q., Zhou, Z.: Graphene-analogous low-dimensional materials. Prog. Mater Sci. **58**, 1244–1315 (2013)
14. Butler, S.Z., Hollen, S.M., Cao, L., Cui, Y., Gupta, J.A., Gutiérrez, H.R., Heinz, T.F., Hong, S.S., Huang, J., Ismach, A.F., Johnston-Halperin, E., Kuno, M., Plashnitsa, V.V., Robinson, R.D.: Progress, challenges, and opportunities in two-dimensional materials beyond graphene. ACS Nano **7**, 2898–2926 (2013)
15. Xu, M., Liang, T., Shi, M., Chen, H.: Graphene-like two-dimensional materials. Chem. Rev. **113**, 3766–3798 (2013)
16. Liang, T., Sawyer, W.G., Perry, S.S., Sinnott, S.B., Phillpot, S.R.: First-principles determination of static potential energy surfaces for atomic friction in MoS_2 and MoO_3. Phys. Rev. B **77**, 104105 (2008)
17. Onodera, T., Morita, Y., Nagumo, R., Miura, R., Suzuki, A., Tsuboi, H., Hatakeyama, N., Endou, A., Takaba, H., Dassenoy, F., Minfray, C., Joly-Pottuz, L., Kubo, M., Martin, J.M., Miyamoto, A.: A computational chemistry study on friction of h-MoS_2. Part II. Friction anisotropy. J. Phys. Chem. B **114**, 15832–15838 (2010)
18. Blumberg, A., Keshet, U., Zaltsman, I., Hod, O.: Interlayer registry to determine the sliding potential of layered metal

dichalcogenides: the case of 2H-MoS_2. J. Phys. Chem. Lett. **3**, 1936–1940 (2012)
19. Cahangirov, S., Ataca, C., Topsakal, M., Sahin, H., Ciraci, S.: Frictional figures of merit for single layered nanostructures. Phys. Rev. Lett. **108**, 126103 (2012)
20. Levita, G., Cavaleiro, A., Molinari, E., Polcar, T., Righi, M.C.: Sliding properties of MoS_2 layers: load and interlayer orientation effects. J. Phys. Chem. C **118**, 3809–13816 (2014)
21. Wang, C., Li, H.S., Zhang, Y.S., Sun, Q., Jia, Y.: Effect of strain on atomic-scale friction in layered MoS_2. Tribol. Int. **77**, 211–217 (2014)
22. Marom, N., Bernstein, J., Garel, J., Tkatchenko, A., Joselevich, E., Kronik, L., Hod, O.: Stacking and registry effects in layered materials: the case of hexagonal boron nitride. Phys. Rev. Lett. **105**, 046801 (2010)
23. Wang, L.F., Ma, T.B., Hu, Y.Z., Wang, H., Shao, T.M.: Ab initio study of the friction mechanism of fluorographene and graphene. J. Phys. Chem. C **117**, 12520–12525 (2013)
24. Deng, Z., Smolyanitsky, A., Li, Q., Feng, X.Q., Cannara, R.: Adhesion-dependent negative friction coefficient on chemically modified graphite at the nanoscale. Nat. Mater. **11**, 1032–1037 (2012)
25. Smolyanitsky, A., Killgore, J.P.: Anomalous friction in suspended graphene. Phys. Rev. B **86**, 125432 (2012)
26. Park, J.Y., Ogletree, D.F., Thiel, P.A., Salmeron, M.: Electronic control of friction in silicon pn junctions. Science **313**, 186 (2006)
27. Wang, L.F., Ma, T.B., Hu, Y.Z., Wang, H.: Atomic-scale friction in graphene oxide: an interfacial interaction perspective from first-principles calculations. Phys. Rev. B **86**, 125436 (2012)
28. Cahangirov, S., Ciraci, S., Özçelik, V.O.: Superlubricity through graphene multilayers between Ni(111) surfaces. Phys. Rev. B **87**, 205428 (2013)
29. Wang, J.J., Wang, F., Li, J., Wang, S., Song, Y., Sun, Q., Jia, Y.: Theoretical study of superlow friction between two single-side hydrogenated graphene sheets. Tribol. Lett. **48**, 255–261 (2012)
30. Wang, J.J., Wang, F., Li, J., Sun, Q., Yuan, P., Jia, Y.: Comparative study of friction properties for hydrogen- and fluorine-modified diamond surfaces: a first-principles investigation. Surf. Sci. **608**, 74–79 (2013)
31. Ramasubramaniam, A., Naveh, D., Towe, E.: Tunable band gaps in bilayer transition-metal dichalcogenides. Phy. Rev. B **84**, 205325 (2011)
32. Liu, Q., Li, L., Li, Y., Gao, Z., Chen, Z., Lu, J.: Tuning electronic structure of bilayer MoS2 by vertical electric field: a first-principles investigation. J. Phys. Chem. C **116**, 21556–21562 (2012)
33. Kresse, G., Hafner, J.: Ab initio molecular-dynamics simulation of the liquid-metal–amorphous-semiconductor transition in germanium. Phys. Rev. B **49**, 14251–14269 (1994)
34. Kresse, G., Furthmüllerb, J.: Efficiency of ab initio total energy calculations for metals and semiconductors using a plane-wave basis set. Comput. Mater. Sci. **6**, 15–50 (1996)
35. Blöchl, P.E.: Projector augmented-wave method. Phys. Rev. B **50**, 17953–17979 (1994)
36. Kresse, G., Joubert, D.: From ultrasoft pseudopotentials to the projector augmented-wave method. Phys. Rev. B **59**, 1758–1775 (1999)
37. Perdew, J.P., Burke, K., Ernzerhof, M.: Generalized gradient approximation made simple. Phys. Rev. Lett. **77**, 3865–3868 (1996)
38. Monkhorst, H.J., Pack, J.D.: Special points for Brillonin-zone integrations. Phys. Rev. B **13**, 5188–5192 (1976)
39. Grimme, S.: Semiempirical GGA-type density functional constructed with a long-range dispersion correction. J. Comput. Chem. **27**, 1787–1799 (2006)
40. Neugebauer, J., Scheffler, M.: Adsorbate-substrate and adsorbate-adsorbate interactions of Na and K adlayers on Al(111). Phys. Rev. B **46**, 16067–16080 (1992)